remains near the critical energy state for a period of time, angular rate sensors could show several changes of sign for ω_3. However, this situation should be avoidable through appropriate selection of devices and sensors.

It can be seen that the size and location of the control masses are important quantities, as these dictate the size of the steps in the energy state and critical energy level. Sufficient change in I_{12} must be generated to insure that after weight shift T^* does not reach I_{12} before ω_3 changes sign. Also, the dissipative mechanism used in this simulation is especially effective as ω_3 changes sign. Thus, as the weights are returned with ω_3 going from minus to plus, the added energy is quickly dissipated. Different damping systems might require that care be taken not to drive the energy to an excessively high value after the weights have been returned to their original positions. No attempt has been made here to quantitatively describe these limiting parameter values for this situation.

Conclusions

The results of this study indicate that a spinning body can be reoriented from spin about the minor to spin about the major axis using passive energy dissipation, utilizing one of three methods to control the final spin direction. Of these three methods, two (the moving masses and spinning of internal inertia) result in no change in the inertial angular momentum vector. Thus, final state is completely dictated by the initial configuration. The mass expulsion method, while probably the most flexible, generates some change in the angular momentum vector, which would have to be evaluated after completion of the reorientation maneuvers.

References

[1] Likins, P. W. and Bouvier, H. K., "Attitude Control of Nonrigid Spacecraft," *Astronautics and Aeronautics*, Vol. 9, No. 5, May 1971, pp. 64–71.

[2] Kaplan, M. H. and Beck, N. M., "Attitude Dynamics and Control of Apogee Motor Assembly with Paired Satellites," *Journal of Spacecraft and Rockets*, Vol. 9, No. 6, June 1972, pp. 410–415.

[3] Hazeltine, W. R., "Passive Damping of Wobbling Satellites: General Stability Theory and Example," *Journal of the Aerospace Sciences*, Vol. 29, No. 5, May 1962, pp. 543–549, 557.

[4] Baines, D. J., "A Satellite Rotational Kinetic Energy Dissipator," *Journal of Spacecraft and Rockets*, Vol. 6, No. 7, July 1965, pp. 850–853.

[5] Hopper, F. W., "Active Precession Control for Spin Stabilized Space Vehicles," AIAA Paper 71-952, Hempstead, N.Y., 1971.

[6] Likins, P. W., "Effects of Energy Dissipation on the Free Body Motions of Spacecraft," TR 32-860, July 1966, Jet Propulsion Lab. Pasadena, Calif.

DECEMBER 1973 J. SPACECRAFT VOL. 10, NO. 12

Motion of a Dual-Spin Satellite during Momentum Wheel Spin-Up

S. Sen* and P. M. Bainum†
Howard University, Washington, D.C.

The stability of a dual-spin satellite system during the momentum wheel spin-up maneuver is treated both analytically and numerically. The dual-spin system consists of a slowly rotating main body; a momentum wheel (or rotor) which is accelerated by a torque motor to change its initial angular velocity relative to the main part to some high terminal value; and a nutation damper. A closed form solution for the case of a symmetrical satellite indicates that when the nutation damper is physically constrained from movement (i.e., by use of a mechanical clamp) the magnitude of the vector sum of the transverse angular velocity components remains bounded during the wheel spin-up under the influence of a constant motor torque. The analysis is extended to consider such effect as the motion of the nutation damper during spin-up, and the effect of a nonsymmetrical mass distribution. An approximate analytical solution using perturbation techniques is developed for a slightly asymmetric main spacecraft. For the case of small mass asymmetry the system behaves similarly to the case of a symmetrical satellite; whereas for large asymmetry the frequency change in both the angular velocity components is noted. When the effect of the misalignment of the main spacecraft (spin) principal axis from the geometrical (polar) axis of symmetry is considered, a problem of stability could arise due to the large initial amplification of the system nutation angle.

Nomenclature

A, B, C = moments of inertia about X, Y, Z axes, respectively, for the main body
A', B', C' = A, B, C + rotor contribution
$\bar{A}, \bar{B}, \bar{C}$ = A', B', C' + damper contribution
$C(x,b)$ = Boehmer integral appearing in approximate perturbation solution
$I(1), I(2), I(3)$ = functions appearing in the particular part of the approximate perturbation solution
I_{ij} = moment of inertia tensor of satellite main body $i, j = x, y, z$
K = restoring spring constant of the torsion wire support
k = damping rate constant
l = height of damper plane above X, Z plane
L_i = applied external torque about the quasi-coordinate axis of symmetry
L_{R_y} = rotor torque
M = the mass of the main satellite
$\bar{M}$ = the total system mass = $M + \sum_i^n m_i$

Presented as Paper 73-142 at the AIAA 11th Aerospace Sciences Meeting, Washington, D.C., January 10–12, 1973; submitted January 16, 1973; revision received July 9, 1973. This research was supported by NASA Grant NGR 09-011-039.

Index category: Spacecraft Attitude Dynamics and Control.

* Graduate Student, Department of Mechanical Engineering; presently, Associate Engineer, Avco Systems Division, Seabrook, Md. Student Member AIAA.

† Associate Professor of Aerospace Engineering. Member AIAA.

m = the pendulum end mass
r_o = the distance from the nominal spin (Y) axis to the pendulum hinge point
r_1 = the length of the pendulum
$S(x,b)$ = Boehmer integral appearing in approximate perturbation solution
s = spin rate of rotor relative to main body
t = time
X, Y, Z = principal axes of main satellite
$\Gamma(b, ix)$ = incomplete Gamma function with complex argument
γ = I_{xz}
ϕ_i = damper displacement angle
ω_i = angular velocities about the X, Y, Z axes, respectively (i, = x, y, z)

Introduction

HASELTINE,[1] Likins,[2] and Bainum et al.[3] have investigated the motion of spinning satellites with nutation damping together with attitude stability criteria. A dual-spin spacecraft may be considered to consist of two parts constrained so that the relative motion between them is restricted to a common direction fixed in both bodies. Such a system can resist the effects of external torques because of the combined resultant momentum of the system, even though one of the parts may be rotating very slowly (or even with zero inertial angular velocity). A basic result of dual-spin attitude stabilization studies is that the system, depending on the spin rate and the amount and location of the dampers, may be stable in spin about an axis of minimum moment of inertia.[3]

Since 1962, when the feasibility of a dual-spin satellite system was demonstrated with the Orbiting Solar Observatory I (OSO-I), the dual-spin concept has been applied to other satellite systems including the Small Astronomy Satellite-A (SAS-A), the TIROS-M Meteorological Satellite, the TACSAT Satellite as well as the advanced versions of the OSO-series. The stability theory and design of dual-spin satellites with various types of nutation damping systems was described at a symposium on the attitude stabilization and control of dual-spin satellites.[4] Considerable attention has also been made in the recent literature to the dynamics and stability of various types of dual-spin systems with and without energy dissipation on both the high spinning part (rotor or momentum wheel) and the despun portion (or main body).[2,5]

In all of these previous analyses of dual-spin systems it was assumed that the rotor spins at a constant relative angular rate with respect to the main part. Of interest in this investigation is to include the effects of a variable rate of relative rotation such as may be encountered during the deliberate spin-up maneuver of the momentum wheel. This can be accomplished by an onboard torque motor which accelerates the wheel until the desired relative spin rate is obtained, at the same time the main part is decelerated as the momentum is transferred between the main part and the wheel.

The dual-spin Small Astronomy Satellite (SAS-A) was launched in Dec. 1970. The satellite was designed to scan the entire celestial sphere to determine the location of X-ray emitting sources relative to the fixed position of the stars. No serious attitude stability problems were encountered during the relatively short time required for wheel spin-up.[6] Because of the experience already gained with this operational system, it was selected as a representative dual-spin system model for the present analysis.

Analysis

A. Equations of Motion for the Case of a Constant Speed Rotor

The elements of the SAS-A attitude control system are shown in Fig. 1. The satellite is comprised of three parts: 1) the primary part of the satellite, assumed to be essentially a right circular cylinder where the nominal spin axis is the body Y-axis, 2) the smaller rotor or momentum wheel which is assumed to be connected near the center of mass of the primary, and assumed to be spinning about the Y-axis with a relative angular velocity, s, with respect to the main spacecraft, and 3) the pendulous type nutation dampers which are connected to the primary part and are constrained to move in a plane $y = l$, perpendicular to the polar axis (only one of these dampers is shown in Fig. 1). It is assumed that the dampers are hinged or pivoted about a torison wire support which offers a restoring (spring) torque in addition to the dissipative torque.[7]

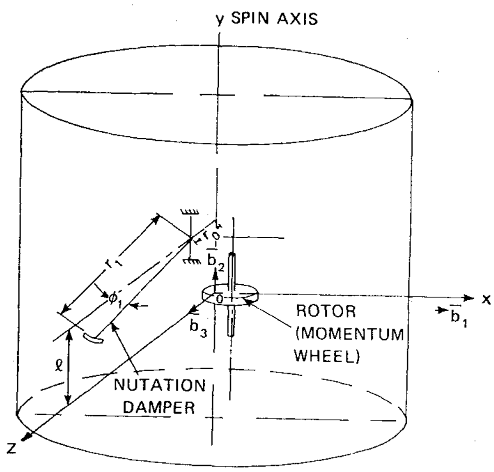

Fig. 1 Elements of SAS-A attitude control system.

The nonlinear equations of motion for a dual-spin satellite with a constant speed rotor can be derived using the quasi-Lagrangian formulation.[8] Under the assumptions that $\omega_x/\omega_y, \omega_z/\omega_y, \dot{\phi}_i/\omega_y$ are small and also with small angle assumptions made relative to the magnitudes of the ϕ_i, the general equations of motion for the case of a constant speed rotor and with only one damper, take the following form:[3]

$$\bar{A}\dot{\omega}_x + (\bar{C} - \bar{B})\omega_y\omega_z - \omega_z I_{R_y} s - 2mr_1 \bar{l}\omega_y \dot{\phi}_1 = L_x \quad (1)$$

$$\bar{B}\dot{\omega}_y + (\bar{A} - \bar{C})\omega_z\omega_x + mr_1(r_0 + r_1)\ddot{\phi}_1 = L_y \quad (2)$$

$$\bar{C}\dot{\omega}_z + (\bar{B} - \bar{A})\omega_x\omega_y - mr_1\bar{l}\ddot{\phi}_1 + mr_1\bar{l}\phi_1\omega_y^2 + I_{R_y}\omega_x s = L_z \quad (3)$$

$$mr_1^2\left(1 - \frac{m}{\bar{M}}\right)\ddot{\phi}_1 - mr_1\bar{l}\dot{\omega}_z + mr_1(r_0 + r_1)\dot{\omega}_y + mr_1\left(r_0 + \frac{mr_1}{\bar{M}}\right)\phi_1\omega_y^2 + mr_1\bar{l}\omega_x\omega_y = -k\dot{\phi}_1 - K\phi_1 \quad (4)$$

where $\bar{l} = lM/\bar{M}$.

B. Eulerian Approach of the Formulation of the Equations of Motion for Variable Speed Rotor

The Eulerian approach is considered here so that it will be possible to distinguish between reaction torques, applied torques, damping torques and external torques. The angular momentum of the main body can be expressed as

$$\bar{L}_M = (A + I_{d_x})\omega_x\bar{i} + (B + I_{d_y})\omega_y\bar{j} + (C + I_{d_z})\omega_z\bar{k} \quad (5)$$

whereas for the rotor

$$\bar{L}_R = I_{R_x}\omega_{R_x}\bar{i} + I_{R_y}\omega_{R_y}\bar{j} + I_{R_z}\omega_{R_z}\bar{k} \quad (6)$$

Using the familiar relationship

$$\left.\frac{d\bar{L}}{dt}\right|_{\text{Space}} = \left.\frac{d\bar{L}}{dt}\right|_{\text{Body}} + \bar{\omega} X \bar{L} = \Sigma\bar{N}$$

the main body equations can be developed as

$$(A+I_{d_x})\dot{\omega}_x+\omega_y\omega_z(C+I_{d_z})-\omega_y\omega_z(B+I_{d_y})=N_{d_x}+R_x \quad (7)$$

$$(B+I_{d_y})\dot{\omega}_y+\omega_z\omega_x(A+I_{d_x})-\omega_z\omega_x(C+I_{d_z})=N_{d_y}+R_y+L_{m_y} \quad (8)$$

$$(C+I_{d_z})\dot{\omega}_z+\omega_x\omega_y(B+I_{d_y})-\omega_x\omega_y(A+I_{d_x})=N_{d_z}+R_z \quad (9)$$

and the rotor equations, similarly:

$$I_{R_x}\dot{\omega}_{R_x}+\omega_y\omega_{R_z}I_{R_z}-I_{R_y}\omega_z\omega_{R_y}=N_{R_x}+R_{R_x} \quad (10)$$

$$I_{R_y}\dot{\omega}_{R_y}+\omega_z\omega_{R_x}I_{R_x}-\omega_x\omega_{R_z}I_{R_z}=N_{R_y}+R_{R_y} \quad (11)$$

$$I_{R_z}\dot{\omega}_{R_z}+\omega_x\omega_{R_y}I_{R_y}-\omega_y\omega_{R_x}I_{R_x}=N_{R_z}+R_{R_z} \quad (12)$$

where I_{R_i} are the principal moments of inertia of rotor, ($i=x$, y,z), I_{d_i} are the moments of inertia of dampers about X,Y,Z, N_{d_i} are the damping torques on the main body, R_i are the reactions (torque) of rotor on main body, N_{R_i} are the (applied) torques acting on the rotor, R_{R_i} are the reactions (torque) of main body on rotor, and L_{m_y} is the motor torque. In Eqs. (7–12) the effect of all external torques (e.g., aerodynamic, solar pressure, gravity-gradient) has been neglected. Substituting first-order expressions for N_{d_i} previously derived,[3] Eqs. (7–9) can be written as

$$(A+I_{d_x})\dot{\omega}_x+\omega_y\omega_z(C+I_{d_z})-\omega_y\omega_z(B+I_{d_y})=2mr_1l\dot{\phi}_1\omega_y+R_x \quad (13)$$

$$(B+I_{d_y})\dot{\omega}_y+\omega_z\omega_x(A+I_{d_x})-\omega_x\omega_z(C+I_{d_z})=-mr_1(r_0+r_1)\ddot{\phi}_1+R_y+L_{m_y} \quad (14)$$

$$(C+I_{d_z})\dot{\omega}_z+\omega_x\omega_y(B+I_{d_y})-\omega_x\omega_y(A+I_{d_x})=mr_1l\ddot{\phi}_1-mr_1l\phi_1\omega_y^2+R_z \quad (15)$$

The assumptions are, that reaction torques are equal and opposite, $R_i=-R_{R_i}$, and the inertia (motor) torques about axes other than the spin axis are zero, i.e., $N_{R_x}=N_{R_z}=0$, but ideally, $N_{R_y}=-L_{m_y}$, i.e., the inertia torque about the spin axis is equal and opposite to the motor torque. Now combining, Eqs. (10) and (13), Eqs. (11) and (14), and Eqs. (12) and (15) and noting that,

$$\omega_{R_y}=\omega_y+s, \quad \omega_{R_z}=\omega_z, \quad \text{and} \quad \omega_{R_x}=\omega_x$$

we obtain

$$\bar{A}\dot{\omega}_x+(\bar{C}-\bar{B})\omega_y\omega_z-\omega_zI_{R_y}s=2mr_1l\dot{\phi}_1\omega_y \quad (16)$$

$$\bar{B}\dot{\omega}_y+(\bar{A}-\bar{C})\omega_z\omega_x+I_{R_y}\dot{s}=-mr_1(r_0+r_1)\ddot{\phi}_1 \quad (17)$$

$$\bar{C}\dot{\omega}_z+(\bar{B}-\bar{A})\omega_x\omega_y+\omega_xI_{R_y}s=mr_1l\ddot{\phi}_1-mr_1l\phi_1\omega_y^2 \quad (18)$$

In addition, the general torque equation for the symmetrical rotor, (i.e., $I_{R_x}=I_{R_z}$) is obtained from Eq. (11),

$$I_{R_y}(\dot{\omega}_y+\dot{s})\approx L_{R_y} \quad (19)$$

where the approximation has been made that the motor torque is much greater than the reaction torque about the Y axis, i.e.,

$$L_{m_y}\approx L_{R_y}\gg R_y$$

When $\dot{s}=0$, then Eqs. (16–18) are identical to Eqs. (1–3).

C. Stability Analysis for the Special Case of an Undamped Symmetrical Satellite

We will consider the system without damping, and a spacecraft symmetrical about the nominal spin axis, i.e., $I_{d_i}=0$, $C=A$, and $I_{R_x}=I_{R_z}$. Under these assumptions Eqs. (16–18) take the following form:

$$A'\dot{\omega}_x+(A'-B')\omega_y\omega_z-\omega_zI_{R_y}s=0 \quad (20)$$

$$B'\dot{\omega}_y+I_{R_y}\dot{s}=0 \quad (21)$$

$$A'\dot{\omega}_z+\omega_x\omega_y(B'-A')+\omega_xI_{R_y}s=0 \quad (22)$$

The general torque equation, Eq. (19) is again

$$I_{R_y}(\dot{\omega}_y+\dot{s})\approx L_{R_y}$$

It should be noted that Eqs. (20–22) are exact with no restrictions on the magnitudes of ω_x and ω_z; also that Eqs. (20–22) and the torque equation are applicable to the general class of symmetrical dual-spin spacecraft in the absence of damping.

After multiplying Eq. (20) by ω_x and Eq. (22) by ω_z and adding then a first integral results as

$$\omega_x^2+\omega_z^2=K_1^2=\text{const} \quad (23)$$

Equation (23) indicates that the amplitude of the vector sum of the transverse angular velocity components is bounded during spin-up. Equation (21) can be integrated directly, to yield

$$\omega_y=-[I_{R_y}s+B'\omega_y(0)+I_{R_y}s(0)]/B' \quad (24)$$

Upon substitution of $\dot{\omega}_y$ from Eq. (21) into Eq. (19),

$$\dot{s}=\frac{L_{R_y}}{I_{R_y}[1-(I_{R_y}/B')]}=c=\text{const} \quad (25)$$

Upon integration of Eq. (25)

$$s=ct+s(0) \quad (26)$$

which states that the relative angular velocity of the rotor, for the case of a symmetrical satellite increases uniformly during spin-up.

Substituting the values of ω_y and s into Eqs. (20) and (22) we can get

$$A'\dot{\omega}_x+\omega_z[P+Q\{ct+s(0)\}]=0 \quad (27)$$

$$A'\dot{\omega}_z-\omega_x[P+Q\{ct+s(0)\}]=0 \quad (28)$$

where

$$P=\{(A'-B')[\omega_y(0)B'+I_{R_y}s(0)]\}/B'$$

$$Q=[(A'-B')(-I_{R_y})]/B'-I_{R_y}$$

Equations (27) and (28) are of the form

$$\dot{\omega}_x+M'(t)\omega_z=0 \quad (29)$$

$$\dot{\omega}_z-M'(t)\omega_x=0 \quad (30)$$

where

$$M'=\{P+Q[ct+s(0)]\}/A'$$

If we let

$$\tau=\int M'\,dt$$

then Eqs. (29) and (30) may be written

$$d\omega_x/d\tau+\omega_z=0 \quad (31)$$

$$d\omega_z/d\tau-\omega_x=0 \quad (32)$$

which is just the equation of the harmonic oscillator and has the solution

$$\omega_x=K_1\cos\tau=K_1\cos\int_0^t M'dt \quad (33)$$

$$\omega_z=K_1\sin\tau=K_1\sin\int_0^t M'dt \quad (34)$$

From consideration of Eqs. (33) and (34) it is apparent that

$$\omega_x^2+\omega_z^2=K_1^2 \quad (35)$$

which compares directly with the first integral, Eq. (23).

When the nutation damper is physically constrained from movement, the magnitude of vector sum of the transverse angular velocity components remains constant during wheel spin-up under the influence of a constant motor torque. The stability criteria for this system is based on the magnitude of the transverse components of the angular velocity. If the transverse components of the angular velocity do not exceed the initial values, then it is assumed that no serious stability problems would be encountered. The implication of Eq. (35) is the boundedness of this motion during spin-up,

D. Effects of the Misalignment of the Principal Axes from the Geometrical Axes

For the actual SAS-A spacecraft there is a misalignment of the principal main body axes from the geometrical (X, Y, Z) axes. In addition, if the rotor is not perfectly mass balanced there may also be a misalignment of the rotor principal axes from the geometrical axes. To consider these possibilities the first-order nonlinear equations of motion were developed for both the main body and rotor, as before, but now including all the cross products of inertia terms for both the main body and rotor as referenced to the X, Y, Z system. The main body and rotor equations may be combined as before and expanded to include first-order small amplitude nutation damping effects.[3] The resulting first-order nonlinear equations in the coordinates $\omega_x, \omega_y, \omega_z$, s, and ϕ_1, are given in Ref. 9.

Equations for the general case where all (or most) of the cross product terms appear cannot be readily solved analytically and must be evaluated by numerical integration. However, these equations will be considered for a special case which is representative of some of the numerical cases studied later in this paper.

Special case

The system will be considered for the case where $I_{xz} = I_{zx} = \gamma$, $I_{xy} = I_{yz} = 0$, $C' = A'$, $I_{R_{zz}} = I_{R_{xx}}$ and all effects of rotor axes misalignment will be neglected. When it is also assumed that $\omega_x/\omega_y \ll 1$, $\omega_z/\omega_y \ll 1$, $\gamma \ll A'$ and $\gamma \ll B'$, the equations can be written, for the case of no damping, as

$$A'\dot{\omega}_x + (A' - B')\omega_y\omega_z - \omega_z I_{R_{yy}} s = \gamma(\dot{\omega}_z + \omega_x\omega_y) \quad (36)$$

$$B'\dot{\omega}_y + I_{R_{yy}}\dot{s} = 0 \quad (37)$$

$$A'\dot{\omega}_z + (B' - A')\omega_x\omega_y + \omega_x I_{R_{yy}} s = \gamma(\dot{\omega}_x - \omega_y\omega_z) \quad (38)$$

$$I_{R_{yy}}(\dot{\omega}_y + \dot{s}) \approx L_{R_y} \quad (39)$$

It should be recalled that $A' = A + I_{R_{xx}}$ and similarly for B'. This case is dynamically similar to that of a spacecraft having no misalignment in its principal axes but a small difference (2γ) between each of its moments of inertia about the two transverse principal axes.[9]

An approximate solution to Eqs. (36–39) using perturbation techniques will be developed here. Equations (37) and (39) in the variables ω_y and s correspond to Eqs. (21) and (19), respectively, previously developed. These solutions can be represented as

$$s = ct + s(0) \quad (40)$$

$$\omega_y = \omega_y(0) - c_1 t \quad (41)$$

where

$$c_1 = I_{R_{yy}}c/B'$$

After substituting Eqs. (40) and (41) into Eqs. (36) and (38) for the case where $s(0) = 0$, there results

$$A'\dot{\omega}_x + (P + Qct)\omega_z = \gamma[\dot{\omega}_z + \omega_x(\omega_y(0) - c_1 t)] \quad (42)$$

$$A'\dot{\omega}_z - (P + Qct)\omega_x = \gamma[\dot{\omega}_x - \omega_z(\omega_y(0) - c_1 t)] \quad (43)$$

where P and Q have been previously defined after Eq. (28).

For the case where $\gamma \ll A'$ and $\gamma \ll |B' - A'|$ a solution using perturbation techniques may be developed by substituting the zeroth-order solutions for ω_x and ω_z, Eqs. (33) and (34), into the right-hand side of Eqs. (42) and (43). The zeroth-order solutions can be represented by

$$\omega_{x_0} = K_1 \cos(x + K_2) \quad (44)$$

$$\omega_{z_0} = K_1 \sin(x + K_2) \quad (45)$$

where

$$x = x(t) = \left|\frac{Qc}{A'}\right| \frac{(t+a)^2}{2}$$

Equation (42) may be differentiated term by term with respect to time and $\dot{\omega}_z$ appearing on the left side eliminated by using (43) to yield

$$A'\ddot{\omega}_x + \frac{[P + Qct]}{A'}\left\{\omega_x[P + Qct] + \frac{\gamma}{A'}[\dot{\omega}_{x_0} - \omega_{z_0}(\omega_y(0) - c_1 t)]\right\} + Qc\omega_z = \gamma\{\ddot{\omega}_{z_0} + [\omega_y(0) - c_1 t]\dot{\omega}_{x_0} - c_1\omega_{x_0}\} \quad (46)$$

After elimination of ω_z by using Eq. (42) and algebraic simplification of all terms appearing with the coefficient "γ", noting that

$$\dot{x} = |Qc|(t + a)/A', \; \dot{\omega}_{x_0} = -\omega_{z_0}\dot{x}, \; \dot{\omega}_{z_0} = \omega_{x_0}\dot{x}$$

and $a = P/Qc$, there results

$$\ddot{\omega}_x - \frac{\dot{\omega}_x}{t+a} + \left(\frac{Qc}{A'}\right)^2 (t+a)^2\omega_x = -\frac{\gamma\omega_{x_0}}{A'}\left[\frac{\omega_y(0) + c_1 a}{t+a}\right] \quad (47)$$

Following the analogous procedure beginning with Eq. (43) and eliminating $\dot{\omega}_x$ and ω_x terms on the left side, a second-order differential equation in ω_z may be obtained

$$\ddot{\omega}_z - \frac{\dot{\omega}_z}{t+a} + \left(\frac{Qc}{A'}\right)^2 (t+a)^2\omega_z = \frac{\gamma\omega_{z_0}}{A'}\left[\frac{\omega_y(0) + c_1 a}{t+a}\right] \quad (48)$$

It is clear that the solutions to the homogeneous parts of Eqs. (47) and (48) are the same as developed previously, namely Eqs. (33) and (34). The particular solution can be obtained by using the method of the variation of parameters.[10] It is convenient to write the complementary solutions as

$$\omega_{x_h} = K_1' \cos x + K_2' \sin x \quad (49)$$

$$\omega_{z_h} = -K_2' \cos x + K_1' \sin x \quad (50)$$

where

$$K_1' = K_1 \cos K_2, \; K_2' = -K_1 \sin K_2$$

The particular soution for ω_x is assumed to have the form

$$\omega_{x_p} = u_1(t)K_1' \cos x + u_2(t)K_2' \sin x \quad (51)$$

subject to the constraint that

$$\dot{u}_1 K_1' \cos x + \dot{u}_2 K_2' \sin x = 0 \quad (52)$$

After differentiating Eq. (51) term by term with respect to time the two equations may be solved simultaneously for $\dot{u}_1$ and $\dot{u}_2$ with the result

$$\dot{u}_1 = \frac{K_3 \sin 2x}{4x} + \frac{K_3 K_2'}{2K_1'}\frac{\sin^2 x}{x} \quad (53)$$

$$\dot{u}_2 = -\frac{K_3 K_1'}{2K_2'}\frac{\cos^2 x}{x} - \frac{K_3 \sin 2x}{4x} \quad (54)$$

The integration of these equations may be facilitated by noting that

$$dt = [A'/2|Qc|]^{1/2} x^{-1/2} dx \quad (55)$$

and performing the integration with respect to x.

The integration is accomplished by using relationships in Sec. 2.632 of Ref. 11 which are valid for $x > 0$ and $a = P/Qc > 0$. These integrals involve products of exponential functions with incomplete gamma functions. It should be noted that the incomplete gamma function with a complex argument, $\Gamma(b,ix)$, can be related to the Boehmer integrals $C(x,b)$ and $S(x,b)$ according to[12]

$$\Gamma(b,ix) = e^{i\pi b/2}[C(x,b) - iS(x,b)] \tag{56}$$

and

$$\Gamma(b,-ix) = e^{-i\pi b/2}[C(x,b) + iS(x,b)] \tag{57}$$

where

$$C(x,b) = \int_x^\infty t^{b-1} \cos t \, dt \tag{58}$$

$$S(x,b) = \int_x^\infty t^{b-1} \sin t \, dt \tag{59}$$

(for the real part of $b < 1$) and the Boehmer integrals may be evaluated by the following series[12]

$$C(x,b) = \Gamma(b) \cos\left(\frac{b\pi}{2}\right) - \sum_{m=0}^{\infty} \frac{(-1)^m x^{2m+b}}{(2m)!(2m+b)} \tag{60}$$

$$S(x,b) = \Gamma(b) \sin\left(\frac{b\pi}{2}\right) - \sum_{m=0}^{\infty} \frac{(-1)^m x^{2m+1+b}}{(2m+1)!(2m+1+b)} \tag{61}$$

It can be verified that for the integrals appearing in Eqs. (53) and (54), $b = -\frac{1}{2}$ and no imaginary terms will appear in the final answer. After some algebra and simplification, utilizing Ref. 11, Eqs. (56) and (57), it can be shown that

$$u_1(t) = (K_4/K_1')\{I(1) \cos K_2 + I(2) \sin K_2 - I(3) \sin K_2\} \tag{62}$$

$$u_2(t) = (K_4/K_2')\{I(1) \sin K_2 - I(2) \cos K_2 - I(3) \cos K_2\} \tag{63}$$

where

$$K_4 = \frac{K_3 K_1 (A'/2|Qc|)^{1/2}}{2}; \qquad K_3 = \frac{\gamma[\omega_y(0) + c_1 a]}{A'}$$

$$I(1) = -\frac{1}{(2)^{1/2}}\left[S\left(2x, -\frac{1}{2}\right)\Big|_{x=0}^{x}\right];$$

$$I(2) = -\frac{1}{(2)^{1/2}}\left[C\left(2x, -\frac{1}{2}\right)\Big|_{x_t=0}^{x}\right]$$

$$I(3) = -\frac{1}{4}x^{-1/2}\Big|_{x_t=0}^{x}$$

The complete approximate solution for ω_x can then be represented by

$$\omega_x = K_1 \cos(x + K_2) + K_1' u_1(t) \cos x + K_2' u_2(t) \sin x \tag{64}$$

Following the same procedure as explained previously the complete approximate solution for ω_z may be developed as

$$\omega_z = K_1 \sin(x + K_2) - K_2' u_3(t) \cos x + K_1' u_4(t) \sin x \tag{65}$$

where

$$u_3(t) = -(K_4)/(K_2')\{-I(1) \sin K_2 + I(2) \cos K_2 - I(3) \cos K_2\}$$

$$u_4(t) = (K_4)/(K_1')\{I(1) \cos K_2 + I(2) \sin K_2 + I(3) \sin K_2\}$$

The constants K_1 and K_2 can be related to the initial conditions on $\omega_x, \omega_z, \dot{\omega}_x$, and $\dot{\omega}_z$.

Numerical Results

Since the SAS-A dual-spin spacecraft system was used as the basis for the mathematical model in the previous analyses, the following SAS-A spacecraft design parameters were used in the numerical calculations:[13] $s = 209$ rad/sec; $\omega_y = 0.5$ rad/sec; $M = 132.33$ kg; $B = 28.54$ kg-m^2; $A = C = 27.00$ kg-m^2; $L_{R_y} = 0.8$ oz-in. (Ref. 14).

A. Calculations of Spin Rate of Rotor during Spin-Up for the Symmetrical Satellite

The spin rate of the rotor can be calculated using Eqs. (24–26). Upon substitution of the values of the L_{R_y}, I_{R_y} and B' into Eq. (25), $\dot{s} = c = 0.49171863$ rad/sec^2, and the time for spin-up obtained from Eq. (26) is 425 sec (compared to the orbital period of approximately 90 min).

During spin-up for the symmetrical satellite without damping, Eq. (24) can be used to calculate the change of main body angular velocity about the spin axis. Substituting the values of I_{R_y}, B', and s we obtain, $\omega_y - \omega_y(0) = 0.8068922$ rpm. In the actual SAS-A Satellite, its spin rate was observed to be 5 rpm immediately after launch. The wheel was then uncaged and accelerated. This resulted in a decrease in satellite spin rate to about 4 rpm.[6] This change in observed spin rate during spin-up compares with the 0.8068922 rpm in this calculation.

B. Results of Numerical Integration

In this section the results of numerical integration of the nonlinear differential equations of motion for the most general case, i.e., the asymmetrical main part and the symmetrical rotor and also the effect of damping are presented. The numerical integration was carried out using the IBM 1130 and IBM 360/50 electronic computers. The fourth-order Runge-Kutta method was used to integrate the nonlinear differential equations of motion. In all numerical results to be presented here, the main body is assumed to spin with an initial component of 0.5 rad/sec and one of the components of the transverse angular velocity, i.e., $\omega_x(0)$ is chosen initially to be 0.000159 rad/sec. All other initial variables are chosen zero.

In the first case considered, the spin-up for the satellite with a small mass asymmetry on the main spacecraft and damping is shown. Figure 2a, shows an initial increase in the amplitude of one of the components of the transverse angular velocity and a small decay in the amplitude of the transverse angular velocity vector (especially the ω_z component). If this initial rate of decay were projected linearly with time, the resultant nutation time constant would be 31.79 min compared with the nominal maximum time constant of 22.3 min for the SAS-A during nominal performance after the wheel spin-up maneuver. Figure 2b shows a noticeable growth of damper angle amplitude during the time of spin-up. The figure shows a bias around the value 0.006 rad. The reason for the bias can be

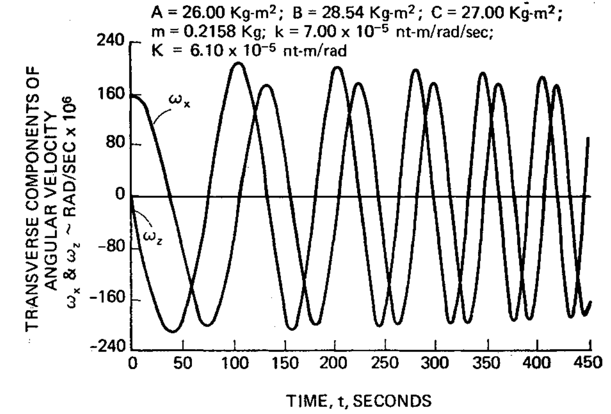

Fig. 2a Time history of the transverse components of main body angular velocity (satellite with small asymmetry in the main body and damping).

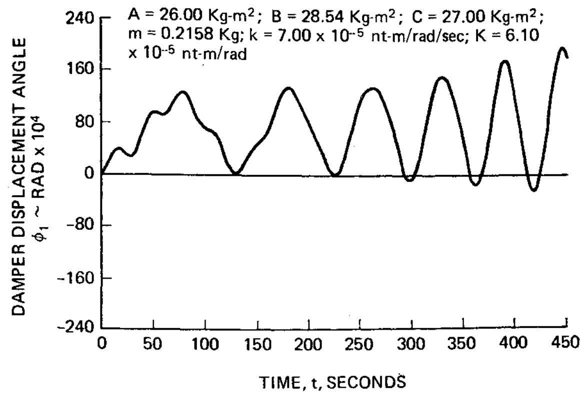

Fig. 2b Nutation damper response during spin-up (satellite with small asymmetry in the main body and damping).

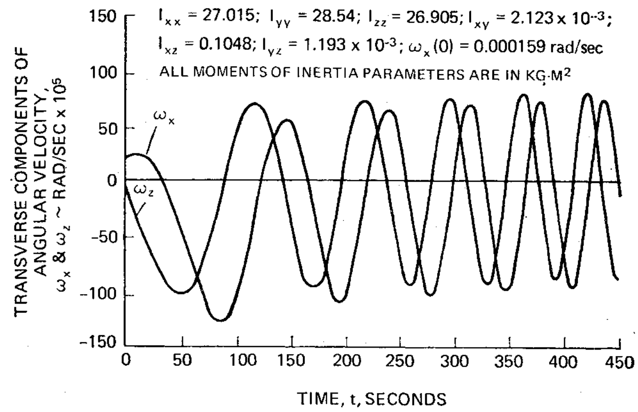

Fig. 4 Time history of the transverse components of main body angular velocity (SAS-A no damping).

explained by the fact that during the derivation of the equations of motion the lateral center of mass shift due to the damper motion was not included.[9,16] When one damper is free to move, this shift could be more noticeable then when a pair of dampers, diametrically opposed in equilibrium, is used. In the actual SAS-A postlaunch performance a small damper bias angle was actually observed.[6,16] One of the causes for this phenomenon was the actual lateral shift in the spacecraft center of mass due to small errors in the final mass balancing prior to launch.[9,16]

In Fig. 3 the initial and final phases of the time history of main body angular velocity components are shown for a spacecraft with a large asymmetry and the nutation damper activated. A significant increase in the frequency of this motion is observed. Since the amplitude of the transverse angular velocity does not exceed the initial value significantly, no serious stability problem would be encountered here.

Figure 4 shows the time history of the transverse components of the main body angular velocity considering the total effect of the misalignment of the principal axes from the geometrical axes of symmetry. It is seen that during the first 100 sec the amplitude of both the transverse components of main body angular velocity increases to approximately 7 times the initial value. After the first cycle of motion, both the components of transverse angular velocity show a decay in their amplitude. Since the stability criteria is based on the boundedness of the transverse components of angular velocity, a problem of stability could be encountered here, especially in the presence of external torques which are initially and continuously acting on the main spacecraft.

A comparison is made between the results of the numerical integration and the approximate solution for the case which is dynamically similar to that of a spacecraft with no misalignment in its principal axes, but a small difference between each of its moments of inertia about the two transverse principal axes [Eqs. (36–39)]. The numerical evaluation of the approximate solutions, Eqs. (64) and (65) for the SAS-A spacecraft during spin-up was performed for a total time interval of 450 sec with a time step of 1 sec. In Fig. 5 the solid curve which is the result of the numerical integration shows a small initial amplification in amplitude of one of the transverse components (ω_x) of main body angular velocity.

No initial amplification can be observed from the results of the approximate solution (shown by dotted lines), but a small change in phase compared to the results of the numerical integration is observed from Fig. 5. The case considered in Fig. 5 could be compared with the case in Fig. 4, where an initial amplification in amplitude of a factor of seven is observed for both the transverse components. By observing the case considered in Fig. 5, it could be concluded that when the nominal spin axis (polar axis) is no longer a principal axis ($I_{xy} \neq 0, I_{yz} \neq 0$) the large amount of initial amplification of the transverse components of main body angular velocity is the

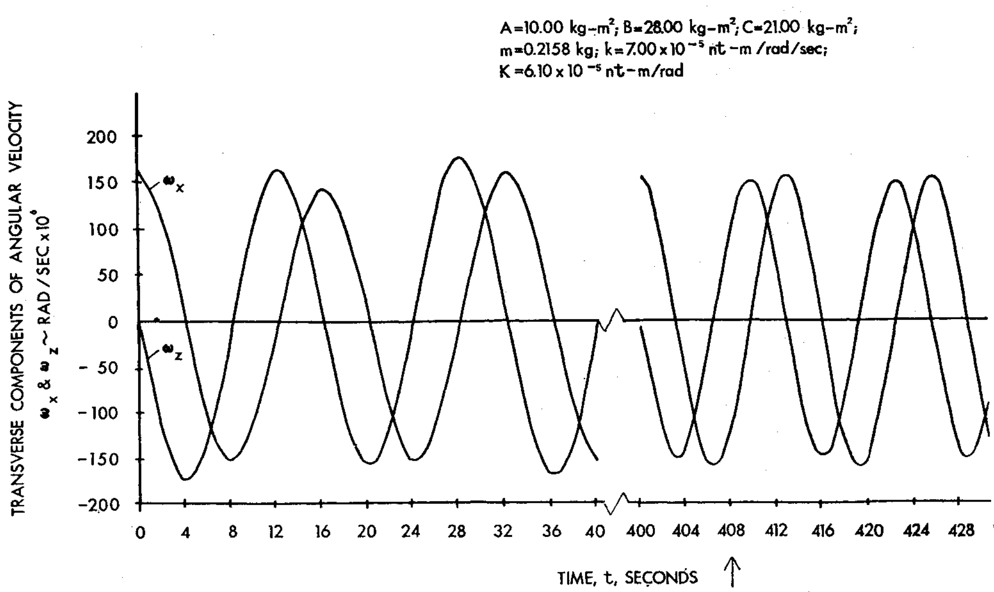

Fig. 3 Time history of the transverse components of main body angular velocity (satellite with large asymmetry in the main body and damping).

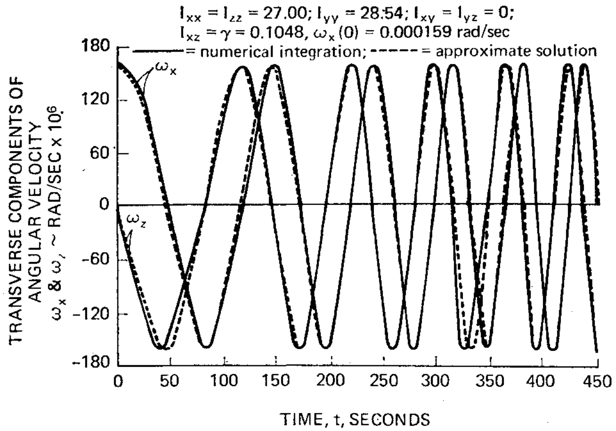

Fig. 5 Time history of the transverse components of main body angular velocity (SAS-A no damping).

result. The amplification is more sensitive to a small misalignment between the principal axis of spin and the nominal spin (geometrical *-yy*) axis, than to small differences between the two transverse moments of inertia. The amplification can further be explained as, when the nominal spin axis is no longer the principal axis, the motor torque has a component perpendicular to the nominal spin vector. This perpendicular component could cause an excitation in the motion about the transverse axis due to the altering nature of the torque component, depending on the relative phasing.

Conclusions

As a result of the present analysis and numerical results the following conclusions can be made:

1) For the case of a symmetrical satellite with no damping the magnitude of the vector sum of the transverse angular velocity remains constant during the wheel spin-up under the influence of a constant motor torque.

2) The effect of the nutation damper during spin-up is significant only for the case of an asymmetry in the main spacecraft, where a small decay in the amplitude of the transverse angular velocity vector is noted. There appears to be little advantage (or disadvantage) in activating the nutation damper for the case of no asymmetry.

3) When the effect of the misalignment of the main spacecraft principal axis from the geometrical (polar) axis of symmetry is considered, a problem of stability could arise due to the large initial amplification of the amplitude of the transverse angular velocity vector.

References

[1] Haseltine, W. R., "Nutation Damping Rates for a Spinning Satellite," *Aerospace Engineering*, Vol. 21, No. 3, March 1962, pp. 10–17.

[2] Likins, P. W., "Attitude Stability Criteria for Dual-spin Spacecraft," *Journal of Spacecraft and Rockets*, Vol. 4, No. 12, Dec. 1967, pp. 1638–1643.

[3] Bainum, P. M., Fuechsel, P. G., and Mackison, D. L., "Motion and Stability of a Dual-spin Satellite with Nutation Damping," *Journal of Spacecraft and Rockets*, Vol. 7, No. 6, June 1970, pp. 690–696.

[4] "Proceedings of the Symposium on Attitude Stabilization and Control of Dual-Spin Spacecraft, Aug. 1–2, 1967," Rept. TR-0158, (3-307-01)-16, Nov. 1967, Aerospace Corp., El Segundo, Calif.

[5] Mingori, D. L., "Effects of Energy Dissipation on the Attitude Stability of Dual-spin Satellites," *AIAA Journal*, Vol. 7, No. 1, Jan. 1969, pp. 20–27.

[6] Fischell, R. E. and Kershner, R. B., "Attitude Control System for a Small Astronomy Satellite," *4th IFAC Symposium on Automatic Control in Space*, Dubrovnik, Yugoslavia, Sept. 1971.

[7] Tossman, B. E., "Variable Parameter Nutation Damper for SAS-A," AIAA Paper 70-972, Santa Barbara, Calif., 1970.

[8] Whitaker, E. T., *A Treatise on the Analytical Dynamics of Particles and Rigid Bodies*, 4th ed., Cambridge Univeristy Press, Cambridge, England, 1937, pp. 41–44.

[9] Bainum, P. M. and Sen, S., "Motion and Stability of a Dual-Spin Satellite During the Momentum Wheel Spin-Up Maneuver," Final Report, NASA Grant NGR 09-011-039, Nov. 1972, Dept. of Mechanical Engineering, Howard Univ., Washington, D.C.

[10] Wylie, C. R., Jr., *Advanced Engineering Mathematics*, 2nd ed., McGraw-Hill, New York, 1960, pp. 99–100.

[11] Gradshteyn, I. S. and Ryzhik, I. M., *Tables of Integrals, Series, and Products*, 4th ed., (Translated from the Russian by Scripta Technica, Inc.), Academic Press, New York, 1965, p. 183.

[12] Bateman Manuscript Project, *Higher Transcendental Functions*, Vol. II, McGraw-Hill, New York, 1953, pp. 133–151.

[13] Fuechsel, P. G., Bainum, P. M., and Grunberger, P. J., "Attitude Motion of a Nutationally Damped Dual-Spin Spacecraft in the Presence of Near-Earth Environment," *Journal of Spacecraft and Rockets*, Vol. 8, No. 9, Sept. 1971, pp. 913–914.

[14] Fountain, G. H. and Philips, B. M., "SAS-A Momentum Wheel," Rep. APL/JHU CP 012, Feb. 1972, Applied Physics Lab., Silver Spring, Md.

[15] Bainum, P. M., Fuechsel, P. G., and Fedor, J. V., "Stability of a Dual-Spin Spacecraft with a Flexible Momentum Wheel," *Journal of Spacecraft and Rockets*, Vol. 9, No. 9, Sept. 1972, pp. 640–646.

[16] Tossman, B. E., "SAS-A Nutation Damper-Flight Observed Bias Angle," Memo S2P-2-410, Jan. 20, 1971, Applied Physics Lab., Silver Spring, Md.